Available online at www.sciencedirect.com
ScienceDirect
Cement and Concrete Research 36 (2006) 1672 – 1678
Cement and Concrete Research

# Effect of short fibers on residual permeability and mechanical properties of hybrid fibre reinforced high strength concrete after heat exposition

Sofren Leo Suhaendi [a,*], Takashi Horiguchi [a]

[a] Department of Civil Engineering, Hokkaido University, Kitaku Kita 13 Nishi 8, Sapporo 060-8628, Japan

Received 25 March 2005; accepted 16 May 2006

**Abstract**

Mechanical and permeability performance of fibre reinforced high strength concrete after heat exposition were evaluated in the experimental study. Cylindrical concrete specimens were exposed to heat with the rate of 10 °C/min of up to 400 °C. In order to study the effect of short fibres on residual performance of heated high strength concrete, polypropylene and steel fibres had been added into the concrete mix. The melting and vaporization of its fibre constituents were found to be responsible for the significant reduction in residual properties of polypropylene fibre reinforced high strength concrete. In terms of non-destructive measurement, UPV test was proposed as a promising initial inspection method for fire damaged concrete structure. Furthermore, the effect of hybrid fibre on the residual properties of heated fibre reinforced high strength concrete was also presented.


*Keywords:* E. High performance concrete; E. Fibre reinforcement; C. Mechanical properties; C. Permeability; E. Durability

## 1. Introduction

Explosive spalling had been considered as a common phenomenon occurring inconsistently when high strength concrete (HSC) was subjected to high temperature [1–3]. Such catastrophic failure was observed after a fire accident erupted inside Chunnel, a tunnel connecting France and England, for approximately 9 h in November 1996. Incorporating high performance concrete reaching compressive strengths of 80 to 100 MPa, the surfaces of tunnel linings were severely damaged exposing steel reinforcement without concrete cover [4]. During thermal exposure, free water would start to vaporize, filling the unoccupied pores, trying to escape inside the concrete matrix [5,6]. Unfortunately, better packing density, smaller and less interconnected pores of HSC would prevent this water vapor from escaping quickly inside the matrix. As temperature increased, build-up of a significant pore pressure was generated and once it exceeded HSC tensile strength, explosive spalling occurred. However, this catastrophic failure mechanism was believed not to be dependent on the build-up of pore pressure alone. Thermal gradient and build-up of strain energy due to thermal stress might also play a secondary role in this explosive spalling mechanism [7].

Recent researches reported that inclusion of polypropylene fibres inside the concrete mix might be considered as an effective way in mitigating explosive spalling failure mechanism [8–10]. Mitigation mechanism was achieved by the melting of polypropylene fibres at 160–170 °C, providing passages for water vapor to escape thus reducing the pore pressure inside HSC under heat exposition [11].

Despite its beneficial contribution in explosive spalling mitigation, residual properties of HSC reinforced by polypropylene fibres would decrease as the consequence of intentionally

Table 1
Short fibres properties

| | Steel | Polypropylene |
|---|---|---|
| Length (mm) | 30 | 6 and 30 |
| Effective diameter (μm) | 600 | 60 |
| Density (kg/m) | 7.8 | 0.9 |
| Shape | Straight, hooked | Straight |

* Corresponding author. Tel./fax: +81 11 706 6180.
*E-mail address:* sofren@eng.hokudai.ac.jp (S.L. Suhaendi).

0008-8846/$ - see front matter © 2006 Elsevier Ltd. All rights reserved.
doi:10.1016/j.cemconres.2006.05.006

Table 2
Mix proportion

| Series | Quantity unit in kg/m$^3$ | | | | $V_f$ (%) | | | | |
|---|---|---|---|---|---|---|---|---|---|
| | Water | Cement | Fine aggregate | Coarse aggregate | Steel fiber | PP fiber | SP [a] (%×$c$) | AE [b] ($A$) | BC [c] ($T$) |
| Plain | 170 | 567 | 955 | 653 | – | – | 1.3 | 7 | – |
| P6-0.25 | 170 | 567 | 951 | 650 | – | 0.25 | 1.3 | 3 | 1 |
| P6-0.5 | 170 | 567 | 947 | 648 | – | 0.5 | 1.3 | 3 | 1 |
| P30-0.25 | 170 | 567 | 951 | 650 | – | 0.25 | 1.7 | 3 | 2 |
| P30-0.5 | 170 | 567 | 947 | 648 | – | 0.5 | 1.9 | 3 | 2 |
| S30-0.25 | 170 | 567 | 951 | 650 | 0.25 | – | 1.3 | 3 | 1 |
| S30-0.5 | 170 | 567 | 947 | 648 | 0.5 | – | 1.3 | 3 | 1 |
| HY-A | 170 | 567 | 943 | 645 | 0.5 | 0.25 | 1.3 | 1 | 4 |
| HY-B | 170 | 567 | 943 | 645 | 0.25 | 0.5 | 1.4 | 1 | 4 |

[a] Superplasticizer.
[b] Air entraining agent, $1A=0.004\%\times c$.
[c] Bubble cutter agent, $1T=0.0002\%\times c$.

generated additional pores. On the contrary, regardless of its effectiveness in mitigating explosive spalling, steel fibres were found able to maintain better residual property of heated HSC [12]. As further possible usage of heated concrete would depend on its residual performance, it is of great importance to know the behavior of fibre reinforced HSC after heat exposition. This experimental study presents the effect of short fibres on residual permeability and mechanical properties of heated HSC.

## 2. Experimental program

### 2.1. Specimens

Concrete specimens were cast using ordinary Portland cement, sandstone with 20 mm nominal maximum size, and river sand with 2.9 fineness modulus. In order to obtain the desired workability (slump flow of 400–600 mm) and air content (5–7%) of the fresh concrete, some chemical admixtures were added into the mix. These chemical admixtures included maleic acid-based superplasticizer, air entraining agent, and bubble cutter agent. Fibres used in the study were steel and polypropylene fibres with the properties shown in Table 1. Polypropylene fibres came in fibrillated form that would disperse inside the concrete mix.

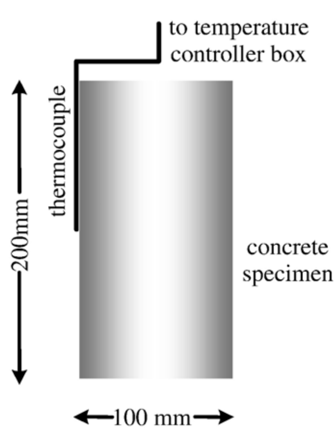


Fig. 1. Specimen inside electric furnace.

Focusing on the effect of short fibres, all series cast had the same water-to-cement ratio of 0.3, sand-to-aggregate ratio of 60%, and water content of 170 kg/m$^3$. The main factor that differentiated each series of the concrete mix was the fibre. The variables included fibre material, fibre length ($l_f$), and fibre volume fraction ($V_f$). Mix proportion of each series of concrete mix is shown in Table 2.

All cylindrical specimens ($\phi$ 100×$H$ 200 mm) were compacted in two layers using a 50 Hz table vibrator. After 28-day curing time, some specimens were heated using a computer-controlled electric furnace. The heating rate was set at 10 °C/min, with peak temperature maintained at 200 °C and 400 °C for 2 h. One thermocouple indicating temperature inside the electric furnace was attached to the side of the specimen, as shown in Fig. 1. After designated heating time elapsed, specimen was taken out and wrapped by ceramic fibre blanket to prevent cracks induced upon cooling. Specimen was then let to cool naturally to room temperature before performing tests, along with the non-heated specimens, in ambient temperature condition.

### 2.2. Performed tests

Prior to loading, ultrasonic pulse velocity test was conducted on the specimen longitudinal direction using white grease as a couplant. For compressive and splitting tensile strength test, loading rate was set at 2 kN/s and 0.2 kN/s, respectively. During compressive strength test, a compressometer was attached to the specimen in order to obtain its modulus of elasticity. Summary of tests performed in the study is given in Table 3.

Table 3
Performed tests

| Test | Parameter | Standard practice |
|---|---|---|
| Slump | – | ASTM C 143 |
| Air content | – | ASTM C 231 |
| UPV | $v$ | ASTM C 597 |
| Compressive | $f'_c, E$ | ASTM C 39, C 469 |
| Tensile | $f_t$ | ASTM C 496 |
| Permeability | $k$ | Modified DIN 1048 |

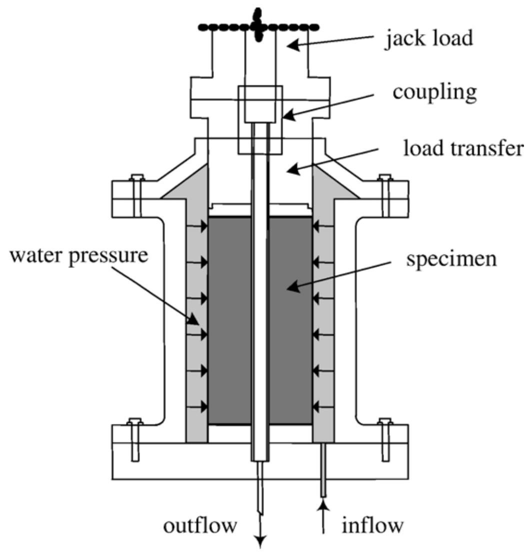


Fig. 2. Permeability cell apparatus.

For the permeability test, the specimen was set inside permeability cell apparatus, as shown in Fig. 2. As soon as the cell was filled with de-aired water, pressure was applied by means of nitrogen gas. Water permeability coefficient was calculated using Darcy's formula, assuming water flow to be continuous and laminar through the concrete specimen.

#### 2.2.1. Input method

A pressure of 1.5 MPa was applied to the specimen for 3 days and water penetration depth was measured after breaking the specimen. Water permeability coefficient was calculated as:

$$k = \frac{d^2}{2ht} \tag{1}$$

where: $d$ = water penetration depth (m), $h$ = water head (m), and $t$ = time (s).

#### 2.2.2. Output method

Application of pressure in this method was greatly reduced compared with former method. Reading of water penetrating concrete specimen was carried out until the steady state flow had been achieved. Water permeability coefficient was then calculated as:

$$k = \frac{\rho \ln\left(\frac{r_0}{r_i}\right)}{2\ \pi\ h} \frac{Q}{P} \tag{2}$$

where: $\rho$ = water density (kg/m$^3$), $r_0$ = specimen radius (m), $r_i$ = central hole radius (m), $Q$ = water outflow (m$^3$/s), $h$ = specimen height (m), and $P$ = water pressure (Pa).

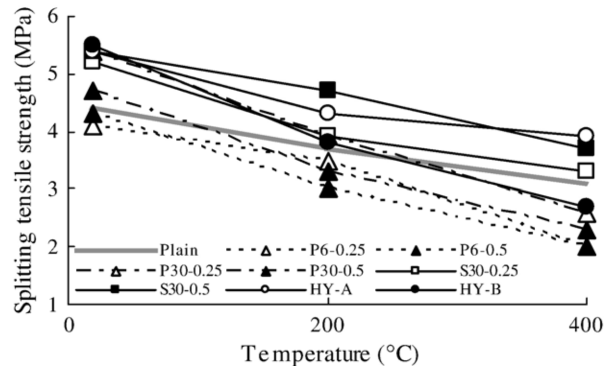


Fig. 4. Tensile strength of heated concrete.

## 3. Results and discussions

### 3.1. Residual mechanical properties

While heating test specimens inside the electric furnace, explosive spalling failure mechanism was observed only on the plain HSC series. Explosive spalling happened at the temperature range of 350–400 °C with an occurrence percentage of 25%. Tests on heated plain concrete were performed on those specimens survived from explosive spalling. Meanwhile, no explosive spalling was found in other series containing polypropylene, steel, or the combination of both fibres.

Obviously, mechanical properties of heated concrete deteriorate with the increasing in maximum heat temperature [13,14], as shown in Figs. 3, 4, and 5. A quite similar degradation trend in compressive strength is shown in Fig. 3 for heated polypropylene fibre reinforced HSC (PFRHSC), steel fibre reinforced HSC (SFRHSC), and hybrid fibre reinforced HSC

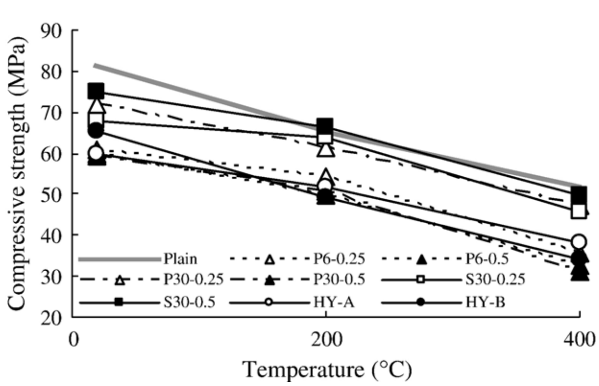


Fig. 3. Compressive strength of heated concrete.

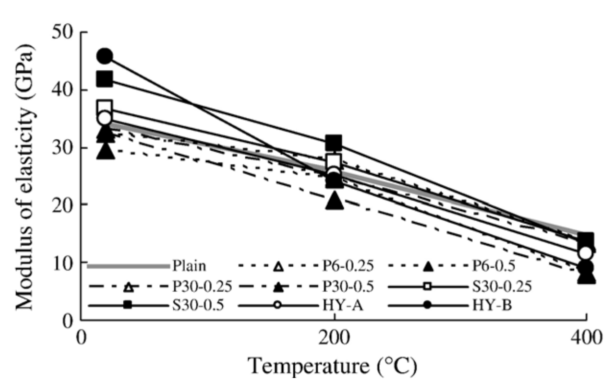


Fig. 5. Modulus of elasticity of heated concrete.

Table 4
Properties reduction of heated concrete

| | Compressive strength | | | Tensile strength | | | Modulus of elasticity | | | Permeability coefficient | | |
|---|---|---|---|---|---|---|---|---|---|---|---|---|
| | Initial (MPa) | Reduction (%) | | Initial (MPa) | Reduction (%) | | Initial (GPa) | Reduction (%) | | Initial (m/s) | Increase (times) | |
| | 20 °C | 200 °C | 400 °C | 20 °C | 200 °C | 400 °C | 20 °C | 200 °C | 400 °C | 20 °C | 200 °C | 400 °C |
| Plain | 81.6 | 20 | 37 | 4.4 | 16 | 30 | 34.3 | 25 | 57 | $2.4\times10^{-12}$ | 19 | 17 |
| P6-0.25 | 60.8 | 11 | 41 | 4.1 | 15 | 51 | 32.4 | 15 | 58 | $3.8\times10^{-12}$ | 45 | 229 |
| P6-0.5 | 60 | 17 | 45 | 4.3 | 30 | 53 | 29.6 | 18 | 72 | $15.5\times10^{-12}$ | 24 | 524 |
| P30-0.25 | 71.9 | 15 | 34 | 5.4 | 28 | 52 | 33.2 | 25 | 60 | $14\times10^{-12}$ | 118 | 2406 |
| P30-0.5 | 59.4 | 15 | 48 | 4.7 | 30 | 51 | 32.4 | 36 | 75 | $17.9\times10^{-12}$ | 344 | 2876 |
| S30-0.25 | 68 | 6 | 33 | 5.2 | 25 | 37 | 36.8 | 26 | 63 | $22.2\times10^{-12}$ | 23 | 42 |
| S30-0.5 | 75.1 | 12 | 34 | 5.4 | 13 | 31 | 41.7 | 27 | 68 | $5.2\times10^{-12}$ | 21 | 140 |
| HY-A | 59.7 | 14 | 36 | 5.4 | 20 | 28 | 34.9 | 27 | 67 | $68.1\times10^{-12}$ | 12 | 26 |
| HY-B | 65.5 | 25 | 48 | 5.5 | 31 | 51 | 45.8 | 47 | 80 | $5.7\times10^{-12}$ | 149 | 1168 |

(HFRHSC). In terms of tensile strength, PFRHSC degrades more rapidly compared with SFRHSC while the combination of its fibres constituent determines the degradation characteristic of HFRHSC. Among the mechanical properties being investigated, modulus of elasticity degrades in a steeper manner compared with compressive and tensile strength. While the reason of this rapid degradation is not clear, the outcome marks the significant loss of stiffness on heated concrete.

Besides the vaporization of free water at 100 °C and loss of hydrates crystallinity [15] that took place in all series, PFRHSC also underwent the melting of its fibres at 160–170 °C and vaporization of fibres at approximately 340 °C. This mechanism, which is preferable during heating exposure, is found to be the cause for significant reduction in properties of PFRHSC.

From Table 4, showing properties reduction of heated concrete, it is interesting to observe that the reduction of PFRHSC in compressive strength and modulus of elasticity after heating at 400 °C depends on polypropylene fibre volume fraction inside the concrete. At this temperature, reduction in compressive strength and modulus of elasticity can reach 48% and 75%, respectively, for HSC containing 0.5% of polypropylene fibres. Reduction in tensile strength is almost the same after heating at 400 °C, approximately 50%, for all HSC containing polypropylene fibres regardless of its fibre volume fraction and fibre length. For SFRHSC, further addition of these fibres inside the concrete mixture will help in keeping the tensile strength of heated concrete at both 200 °C and 400 °C. This may correspond to the effectiveness of steel fibres in bridging cracks induce upon tensile loading, as these fibres do not melt after heat exposition.

In terms of HFRHSC, the reduction in properties will closely depend on the polypropylene fibre volume fraction inside the mixture. Although HY-A and HY-B has the same total fibre volume fraction (=0.75%), reduction in mechanical properties of HY-A is not as rapid as HY-B. While the former mixture contains only 0.25%, the latter mixture contains 0.5% of polypropylene fibres. Reduction in compressive strength, tensile strength, and modulus of elasticity of HY-B can reach 48%, 51%, and 80%, respectively, after heating at 400 °C. This reduction in properties is found almost to be the same as properties reduction of PFRHSC containing 0.5% of polypropylene fibres heated at 400 °C. Hence, proportioning fibre volume fraction of polypropylene and steel fibres will be the crucial factor in achieving the best performance of HFRHSC exposed to high temperature. Further study to identify the most auspicious hybrid fibres mixing proportion will lead to a more durable concrete structure in the aftermath of fire accident.

### 3.2. Non-destructive testing measurement

Generation of pores and cracks resulting from physicochemical changes in cement paste and thermal incompatibility between aggregate and cement paste was believed to be responsible for the deterioration in mechanical properties of heated concrete. Fig. 6 shows the deterioration of concrete quality by means of ultrasonic

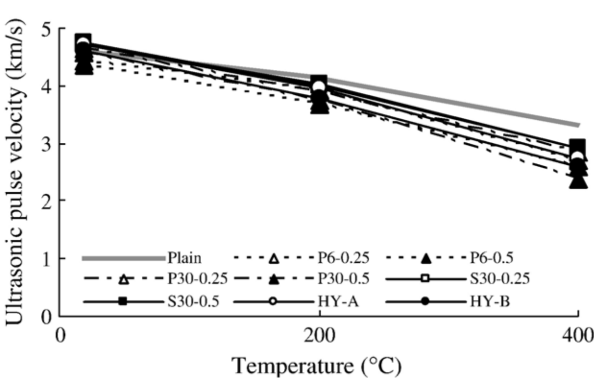


Fig. 6. Ultrasonic pulse velocity of heated concrete.

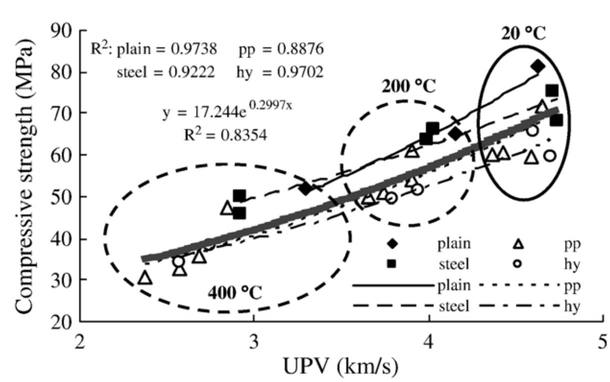


Fig. 7. Correlation between UPV-compressive strength.

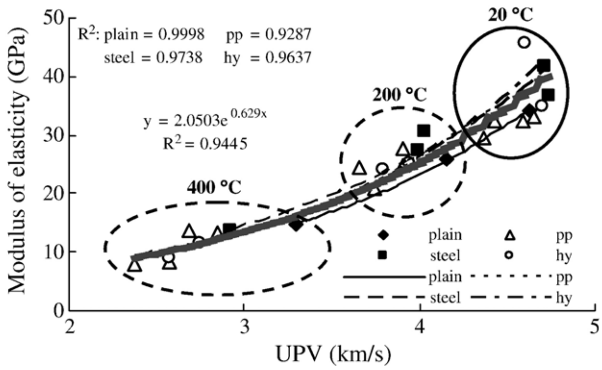


Fig. 8. Correlation between UPV-modulus of elasticity.

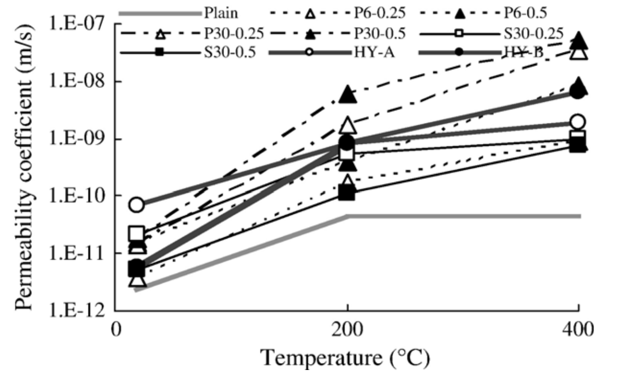


Fig. 10. Water permeability coefficient of heated concrete.

pulse velocity (UPV) measurement. UPV reduces almost proportionally with the increase in maximum heating temperature.

Correlation between UPV-compressive strength, UPV-modulus of elasticity, and UPV-tensile strength of heated concrete is found to give a good agreement between these parameters [16]. In this experimental study, UPV value of 3.3 km/s and 4.2 km/s marks the clustering of the data, shown as ellipsoidal line in Figs. 7–9. While dash ellipsoidal line represents thermally exposed data sets, solid ellipsoidal line represents data sets which were non-exposed thermally. Specimens heated at 400 °C will correspond to UPV less than 3.3 km/s while non-heated ones will correspond to UPV more than 4.2 km/s. Specimens heated at 200 °C will lie between 3.3 and 4.2 km/s.

Using regression analysis including all series, marked by thicker regression line inside the figures, correlation between UPV-compressive strength, UPV-modulus of elasticity, and UPV-tensile strength is given in Eqs. (3) to (5), respectively.

$$f_c = 17.244\ e^{0.2997v} \tag{3}$$

$$E = 2.0503\ e^{0.629v} \tag{4}$$

$$f_t = 1.1054\ e^{0.3222v} \tag{5}$$

where: $f_c$=compressive strength (MPa), $E$=modulus of elasticity (GPa), $f_t$=tensile strength (MPa), and $v$=ultrasonic pulse velocity (km/s).

Separating the data into some particular series (plain HSC, PFRHSC, SFRHSC, and HFRHSC) will even yield in better $R^2$ values, as shown inside the figure. These correlations show that application of non-destructive measurement may be applied in practice making properties inspection of fire damaged concrete quicker and more efficient. Nevertheless, establishment of solid correlation will need more experimental data in the process.

### 3.3. Permeability

Water permeability coefficient of heated concrete increases with the increase in maximum heat temperature, as shown in Fig. 10. Regardless of degradation mechanism characteristic in each series, there are two interesting findings that can be observed from this figure. The first one is that all curves' gradients tend to lessen after 200 °C while the second one is that water permeability coefficient of plain HSC is found to be the lowest among all series, before and after heat exposition [17]. This low water permeability coefficient may imply to the susceptibility of plain HSC to explosive spalling. Starting from initial value of water permeability coefficient, series incorporating fibres slightly showed higher values compared to plain HSC. According to percolation theory, this result might be caused by addition of fibres that effectively generated a percolated pathway inside the cement matrix. However, increment in initial value of water permeability coefficient on fibre reinforced concrete would be insufficient to be considered as the only parameter that would reduce risk of explosive spalling on heated HSC.

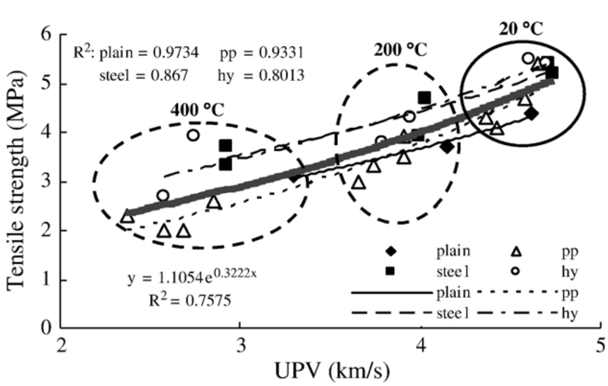


Fig. 9. Correlation between UPV-tensile strength.

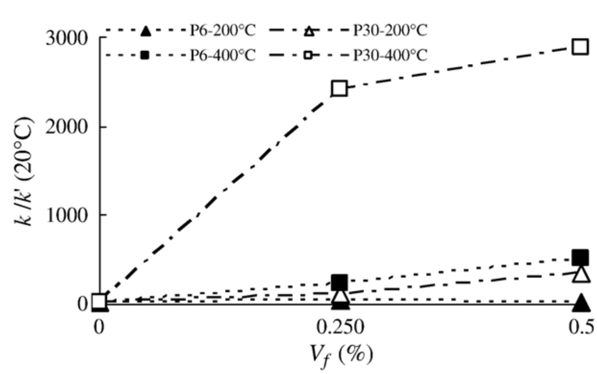


Fig. 11. Effect of fibre volume fraction on residual permeability of heated PFRHSC.

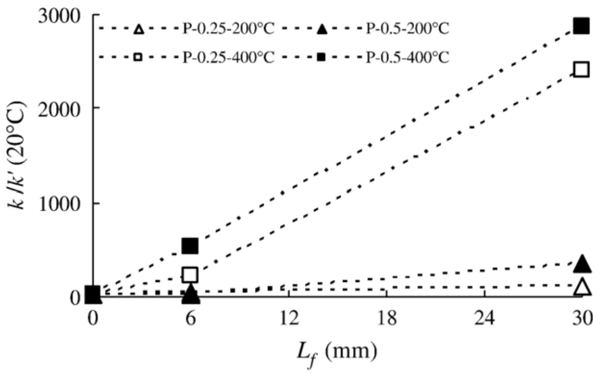


Fig. 12. Effect of fibre length on residual permeability of heated PFRHSC.

Additionally, initial water permeability coefficient of HY-A was found to be the highest following the fact that this series encountered output method instead of input method for its non-heated specimens' permeability test.

Effect of fibre volume fraction and fibre length on permeability performance of PFRHSC will be discussed in the following manner, plotted in Figs. 11–13.

As previously mentioned, explosive spalling mitigation on heated PFRHSC involved the melting of its fibre constituent. While percolation theory stated that more and longer polypropylene fibre would be more effective in creating percolated network inside the concrete matrix [8], permeability performance of heated concrete having more and longer polypropylene fibres surviving explosive spalling would decrease. Figs. 11 and 12 show the effect of fibre volume fraction and fibre length on water permeability coefficient. Inside the figures, *X*-axis will refer to fibre volume fraction or fibre length while *Y*-axis will refer to relative water permeability coefficient, which is the ratio between water permeability coefficient at particular temperature and the one at ambient temperature (20 °C). Water permeability coefficient increases with the increase in volume fraction and length of polypropylene fibres. The latter seems to have a more pronounced effect compared with the former, as longer fibre will create more interconnected pores inside the concrete matrix, making water from outside easily permeating through the concrete. After heating at 400 °C, increase in water permeability coefficient of PFRHSC having 0.25% fibre volume fraction and 30 mm long fibre is found to be one order of magnitude higher than that of PFRHSC having same fibre volume fraction and 6 mm long fibre.

Increase in water permeability coefficient is also found to be higher after heating at 400 °C than at 200 °C. One reason for this may be related to the behavior of polypropylene fibres upon heating. At 200 °C, polypropylene fibre will melt at 160–170 °C with the chance to re-solidify, partially filling the pores once left by these fibres. At 400 °C, polypropylene fibre will vaporize at about 340 °C, leaving no chance for these fibres to re-solidify. Nevertheless, more investigation on microstructure level (i.e. MIP, electron and optical microscopy) should be performed to confirm whether the increase in water permeability coefficient is affected solely by melting or by vaporizing its fibre constituents.

In the case of hybrid fibre, reduction in permeability–durability related performance of HY-A is much less than HY-B after heating at both 200 °C and 400 °C, as shown in Fig. 13. Again, reduction in this property on HFRHSC will be closely related to the proportioning combination of its fibres constituent. More inclusion of polypropylene fibres inside HFRHSC will increase the water permeability coefficient of this concrete type after suffering from heat exposition.

## 4. Conclusions

1. Degradation trend in compressive strength of heated PFRHSC, SFRHSC, and HFRHSC is found to be quite similar while tensile strength of PFRHSC degrades in a more rapid way compared with SFRHSC. For HFRHSC, degradation in tensile strength will be related to proportioning combination of its fibres constituent.
2. With the melting and vaporization of its fibre constituents at 160–170 °C and 340 °C, respectively, PFRHSC loses its mechanical and permeability performance more significantly compared with the other series after heat exposition. Reduction in compressive strength and modulus of elasticity after heat exposition will depend on its fibre volume fraction inside the concrete. Reduction in tensile strength after heating at 400 °C for HSC containing polypropylene fibres reaches 50% regardless of its fibre volume fraction and length.
3. More inclusion of steel fibres will improve tensile strength property of heated HSC. This may indicate the effectiveness of steel fibres in bridging cracks induced upon tensile loading as they do not melt after heat exposition.
4. Close correlation between non-destructive measurement (UPV test) and mechanical properties (i.e. compressive strength, modulus of elasticity, and tensile strength) exist for HSC heated up to 400 °C. In this manner, UPV test can be considered as a promising initial inspection method for fire damaged concrete structure.
5. Compared with fibre volume fraction, length of fibre affects residual permeability performance of heated PFRHSC in a more pronounced way. As longer fibre creates more interconnected pores inside the concrete matrix, substances from outside will be able to penetrate easily through the concrete.
6. In terms of HFRHSC, proportioning combination of steel and polypropylene fibres will be the important factor affecting residual properties of this type of HSC after suffering from heat exposition.

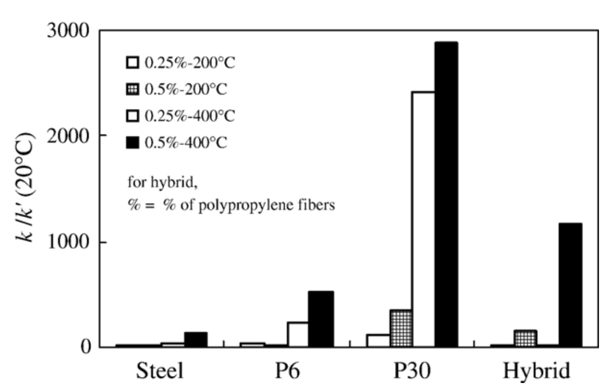


Fig. 13. Reduction in permeability performance of heated fibre reinforced HSC.

## References

[1] C. Castillo, A.J. Durrani, Effect of transient high temperature on high-strength concrete, ACI Mater. J. 87 (1) (1990) 47–53.

[2] L.T. Phan, N.J. Carino, Effects of test conditions and mixture proportions on behavior of high-strength concrete exposed to high temperatures, ACI Mater. J. 99 (1) (2002) 54–66.

[3] P.J.E. Sullivan, A probabilistic method of testing for the assessment of deterioration and explosive spalling of high strength concrete beams in flexure at high temperature, Cem. Concr. Compos. 26 (2004) 155–162.

[4] F.J. Ulm, P. Acker, M. Lévy, The "Chunnel" fire: II. Analysis of concrete damage, J. Eng. Mech. 125 (3) (1999) 283–289.

[5] O. Kontani, S.P. Shah, Pore pressure in sealed concrete at sustained high temperatures, in: K. Sakai, N. Banthia, O.E. Gjørv (Eds.), Concrete Under Severe Conditions: Environment and loading, 1995, pp. 1151–1162.

[6] G.R. Consolazio, M.C. McVay, J.W. Rish III, Measurement and prediction of pore pressures in saturated cement mortar subjected to radiant heating, ACI Mater. J. 95 (5) (1998) 525–536.

[7] L.T. Phan, J.R. Lawson, F.L. Davis, Effects of elevated temperature exposure on heating characteristics, spalling, and residual properties of high performance concrete, Mater. Struct. 34 (2001) 83–91.

[8] P. Shuttleworth, Fire protection of concrete tunnel linings, Proc. 3rd Inter. Conf. Tunnel Fires, 2001, pp. 157–165.

[9] D.P. Bentz, Fibres, percolation, and spalling of high-performance concrete, ACI Mater. J. 97 (3) (2000) 351–359.

[10] T. Horiguchi, T. Sugawara, N. Saeki, Fire resistance of hybrid fibre reinforced high strength concrete, in: M. di Prisco, R. Felicetti, G.A. Plizzari (Eds.), 6th RILEM Sym. on FRC, 2004, pp. 669–678.

[11] P. Kallifa, G. Chéné, C. Gallé, High-temperature behaviour of HPC with polypropylene fibres from spalling to microstructure, Cem. Concr. Res. 31 (2001) 1487–1499.

[12] S.L. Suhaendi, T. Horiguchi, N. Saeki, Permeability of heated fibre reinforced high strength concrete, Proc. JCI 26 (1) (2004) 315–320.

[13] T. Horiguchi, T. Takano, N. Saeki, T.D. Lin, Effect of fibre reinforcement on residual properties of high strength concrete under elevated temperature, ACI SP-209 (2002) 53–64.

[14] M. Li, C.X. Qian, W. Sun, Mechanical properties of high-strength concrete after fire, Cem. Concr. Res. 34 (2004) 1001–1005.

[15] W.M. Lin, T.D. Lin, L.J. Powers-Couche, Microstructures of fire-damaged concrete, ACI Mater. J. 93 (3) (1996) 199–205.

[16] S. Popovics, Analysis of the concrete strength versus ultrasonic pulse velocity relationship, Mater. Eval. 59 (2) (2001) 123–129.

[17] I. Janotka, L. Bágel, Pore structures, permeabilities, and compressive strengths of concrete at temperatures up to 800 °C, ACI Mater. J. 99 (2) (2002) 196–200.